Carbohydrate Polymers 90 (2012) 60–66

Contents lists available at SciVerse ScienceDirect

Carbohydrate Polymers

journal homepage: www.elsevier.com/locate/carbpol

# Structure of oligosaccharide F21 derived from exopolysaccharide WL-26 produced by *Sphingomonas* sp. ATCC 31555

Wei Jia[a,b], Jin-Song Zhang[b], Yun Jiang[a], Zhi-Yong Zheng[a], Xiao-Bei Zhan[a,*], Chi-Chung Lin[a]

[a] *Key Laboratory of Carbohydrate Chemistry and Biotechnology, School of Biotechnology, Jiangnan University, Wuxi, Jiangsu 214122, China*
[b] *National Engineering Research Center of Edible Fungi, Key Laboratory of Applied Mycological Resources and Utilization of Ministry of Agriculture, Shanghai Key Laboratory of Agricultural Genetics and Breeding, Institute of Edible Fungi, Shanghai Academy of Agricultural Sciences, Shanghai 201403, China*

ARTICLE INFO

*Article history:*
Received 12 February 2012
Received in revised form 19 April 2012
Accepted 21 April 2012
Available online 6 May 2012

*Keywords:*
Exopolysaccharide
*Sphingomonas*
Structural characterization
Oligosaccharide F21
Partial acid hydrolysis
NMR

ABSTRACT

Mild hydrolysis of *Sphingomonas* sp. ATCC 31555 polysaccharide WL-26 afforded a new oligosaccharide, F21. Structural resolution based on sugar and methylation analyses as well as NMR data revealed the oligosaccharide to have the following structure:

β-D-GlcA-(1→4)-α-D-Glc*p*-(1→4)-β-L-Rha*p*-(1→4)-α-D-Man*p*-(1→3)-β-D-Glc*p*-(1→4)-β-L-Rha*p*-(1→3)-α-L-Rha*p*
6
↓
1
α-D-Gal*p*



## 1. Introduction

Microbial polysaccharides have a wide range of industrial applications as aqueous rheological control agents in food products, cosmetics and pharmaceuticals. Among the most versatile is xanthan gum, which can serve as a stabilizer, emulsifier and a selective adsorbent (Balsara et al., 1992). In nature, polysaccharides often occur as capsules around bacterial cells to prevent dehydration or to sequester potential carbon sources and deny access to competing species. Polysaccharides have been the subject of intensive research due to their diversity and novelty in terms of structure and function.

Members of the *sphingan* group of bacterial exopolysaccharides (EPS), produced by various *Sphingomonas* species, have similar basic backbone structures and include gellan (S-60) (Jansson, Lindberg, & Sandford, 1983), S-88 (Jansson, Kumar, & Lindberg, 1986), welan (S-130) (Kwon, Foss, & Rha, 1987) and rhamsan (S-194) (Podolsak, Tiu, Saeki, & Usui, 1996). All of these consist of a linear repeating tetrasaccharide backbone containing rhamnose, glucose, mannose and glucuronic acid with side-chain substituents such as glucose or rhamnose connected by glycosidic bonds (Pollock, 2002). Gellan, produced by *S. paucimobilis*, has the repeating unit [→3)-β-D-Glc*p*(1→4)-β-D-GlcA(1→4)-β-D-Glc*p*(1→4)-α-L-Rha*p*(1→] (Jansson et al., 1983). The native polysaccharide is partially esterified; the 1,3-D-Glc residue can be linked to L-glycerate at C-2 and/or to acetate at C-6, and there is 1 mol of glycerate and 0.5 mol of acetate per repeating unit, respectively (Kuo, Mort, & Dell, 1986). Welan (S-130) has a monosaccharide side-chain at position O-3 of the 4-linked glucose that can be either α-L-rhamnose or α-D-mannose. Approximately two-thirds of the tetrasaccharide units of welan gum contain a terminal α-L-rhamnopynanosyl group, while the remaining one-third has an α-D-mannopynanosyl residue (Jansson & Widmalm, 1994). These unusual structures offer unique functionalities distinct from those of xanthan gum.

Due to the high viscosity of the polysaccharides, analytical techniques involving 1D NMR, 2D NMR and chemical microderivatization combined with mass spectrometry are not always effective in elucidating precise structural features. In such cases, the polysaccharide must first be partially depolymerized using various methods including exposure to heat and light, and treatment with chemical reagents and enzymes (Madras & Chattopadhyay, 2001).

Exopolysaccharide WL-26, produced by *Sphingomonas* sp. ATCC 31555, has a molecular mass of $\sim 1.71 \times 10^6$ Da and exhibits a high viscosity at low concentrations that is stable at high ionic concentrations, various pH values and over a wide range of temperature. Glucose, rhamnose, mannose, galactose and glucuronic acid have

* Corresponding author. Tel.: +86 51 85918299; fax: +86 51 85918299.
*E-mail address:* xbzhan@yahoo.com (X.-B. Zhan).

0144-8617/$ – see front matter © 2012 Elsevier Ltd. All rights reserved.
http://dx.doi.org/10.1016/j.carbpol.2012.04.061

been identified among the monosaccharide components, but additional features and the repeating unit of the EPS have not been characterized. Therefore, we have now degraded WL-26 into fragments of lower molecular weight and viscosity by partial acid hydrolysis, and subjected one of these fragments, an oligosaccharide designated F21, to $^{1}H$, $^{13}C$ and 2D NMR spectroscopy combined with GC–MS. Our data describing the structural features of F21 will provide a better understanding of the overall structure of the native polysaccharide, WL-26.

## 2. Materials and methods

### 2.1. Bacterial strain and culture conditions

*Sphingomonas* sp. ATCC 31555 (formerly classified as an *Alcaligenes* sp.) was grown in a medium consisting of ($L^{-1}$): sucrose 40 g, $NaNO_3$ 0.8 g, yeast powder 3.2 g, $KH_2PO_4$, 2.0 g, $MgSO_4$ 0.1 g and $FeSO_4$ 0.5 g. Exponential phase seed cultures (200 mL) (grown in shake flasks) were used to inoculate 1.8 L fermentation broth contained in a 3-L Braun Biostat C stainless steel reactor (Sartorius Stedim Biotech AG, Tagelswangen, Switzerland). Initially, the culture medium contained 20 g $L^{-1}$ sucrose and a second aliquot of the sugar was added 20 h after inoculation. Culture conditions were as follows: temperature 30 °C, impellor speed 400 rpm, pH 7.0 (adjusted with 0.2 mM NaOH), and dissolved oxygen levels were maintained >20% by adjusting the aeration rate during the growth period.

### 2.2. Extraction and purification of polysaccharide WL-26

Crude polysaccharide WL-26 from the fermentation broth was precipitated by adding 95% (v/v) ethanol until the final alcohol concentration reached 75%. The precipitated crude material was then washed with 75% (v/v) ethanol, resuspended in distilled water to the original volume, precipitated once more with 95% (v/v) EtOH, collected by centrifugation (26,000 × *g*, 20 min, 25 °C), and lyophilized. An aliquot (0.2 g) of lyophilized material was resuspended in 2 L distilled water, centrifuged as before, and the supernatant was concentrated 10-fold under vacuum. This solution was dialyzed (cut-off 8.0–10 kDa) for 4 days against 20 changes of distilled water, concentrated to ~10 mL under reduced pressure at 40 °C and lyophilized to give crude polysaccharide fraction WL-26.

### 2.3. Sugar analyses

Samples (2 mg) were hydrolyzed with 2 M trifluoroacetic acid (TFA) at 110 °C for 4 h, and the resulting monosaccharides were identified by high-performance anion exchange pulsed-amperometric detection chromatography (HPAEC-PAD) using a Dionex LC30 instrument equipped with a CarboPac™ PA20 column (3 mm × 150 mm) (Yang, Zhang, Tang, & Pan, 2005). The column was eluted with the mobile phases A, B and C (consisting of deionized water, 250 mmol/L NaOH and 1 mol/L NaAc, respectively) used in the following combinations (A, B, C): 0–30 min, (99.2:0.8:0), 30–40 min (99.2:0.8:0–79.2:0.8:20), 40–40.1 min (79.2:0.8:20–20:80:0), and 40.1–60 min (20:80:0–99.2:0.8:0). The sample volume, column temperature and flow rate were 25 μL, 30 °C and 0.45 mL/min, respectively. Monosaccharide components and percentage composition were determined using D-Gal, D-Glc, D-Ara, L-Fuc, L-Rha, D-Man, D-Xyl, D-glucuronic acid (GlcA) and galacturonic acid (GalA) standards (Sigma–Aldrich, USA).

### 2.4. Partial acid hydrolysis of WL-26 and isolation of F21

After hydrolyzing 20 mg crude WL-26 in 3 mL of 0.2 M TFA for 2 h at 100 °C, most of the solvent was evaporated off under reduced pressure at 40 °C and residual acid was removed by repeated evaporation with methanol. After adding 2 mL distilled water, insoluble material was removed by centrifugation (see above) and the clear supernatant (~1 mL) was fractionated using a Sephacryl S-100 High Resolution gel column (16 mm × 100 cm) (GE Healthcare, Cardiff., UK). Two peaks were resolved on elution with distilled water, and fractions constituting the first (main peak) were collected, concentrated at 45 °C under vacuum and freeze-dried to yield fraction F21.

### 2.5. Determination of purity and molecular weight

Homogeneity and the molecular weight of F21 were determined by HPLC using a Waters 600 Controller System (Waters 717 plus autosampler, Waters 2996 photodiode array detector, Waters 2414 refractive index detector, Waters in-Line Degasser AF), fitted with a TSKPW superoligo (6.0 mm × 150 mm) gel filtration column. Aliquots (10 μL) of F21 solution (2 mg/mL buffer consisting of 0.1 M $NaH_2PO_4$ and 0.3 M $NaNO_3$, adjusted to pH 7.0 with 0.1 M NaOH) were applied to the column and eluted with the same buffer at a flow rate of 0.5 mL/min. The column was calibrated using Dextrans T-2.5 (25,000 Da), T-1.2 (12,000 Da), T-0.5 (5000 Da) and T-0.1 (1000 Da), D-raffinose (522 Da), D-trehalose (378 Da) and D-mannitol (182 Da) (Sigma–Aldrich, USA), and column and RI detector temperatures were set at 35 °C.

### 2.6. Infrared spectroscopy

Aliquots of F21 (1 mg) were converted into KBr discs and analyzed in a PerkinElmer 599B FT-IR spectrophotometer.

### 2.7. Methylation analysis

Vacuum-dried F21 (2 mg) was dissolved in DMSO (1 mL) and methylated with a solution of 2.5% NaOH in DMSO (1 mL) and $CH_3I$ (0.5 mL) for 30 min at room temperature according to the method of Anumula and Taylor (1992). The reaction mixture was extracted with 0.5 mL $CHCl_3$, the organic phase was washed 3× with 2–3 mL MilliQ water, and the solvent was then removed by evaporation under reduced pressure. Complete methylation was confirmed by the disappearance of the —OH band (3200–3700 $cm^{-1}$) in the IR spectrum. Permethylated polysaccharide was hydrolyzed with HCOOH (88%, 3 mL) at 100 °C for 3 h, evaporated to dryness and further hydrolyzed with 2 M TFA (4 mL) at 110 °C for 4 h. The partially methylated oligosaccharide in the hydrolyzate was reduced with $NaBH_4$ and acetylated with $Ac_2O$, and the resulting mixture of methylated alditol acetates was analyzed by GC–MS using a DB-5MS column (30 m × 0.25 mm × 0.25 μm) and a temperature program consisting of 180–270 °C at 20 °C/min, and held at 270 °C for 25 min (Albersheim, Nevins, English, & Karr, 1967).

### 2.8. NMR analysis

F21 (30 mg) was lyophilized three times in $D_2O$ (0.5 ml), and the $^{1}H$ NMR and $^{13}C$ NMR spectra were determined at 27 °C and 40 °C, respectively in 5-mm tubes using a Varian INOVA 500 NMR spectrometer. $^{1}H$ chemical shifts were referenced to residual HDO at $\delta$ 4.78 ppm (27 °C) as the internal standard. $^{13}C$ chemical shifts were determined in relation to DSS (δ 0.00 ppm) calibrated externally. $^{1}H$–$^{1}H$ correlated spectroscopy (COSY), total correlation spectroscopy (TOCSY), and heteronuclear multiple quantum coherence (HMQC) was used to assign signals. Two-dimensional heteronuclear multiple-bond correlation spectroscopy (HMBC) and dimensional Overhauser effect spectroscopy (NOESY) were used to assign inter-residue linkages and sequences.

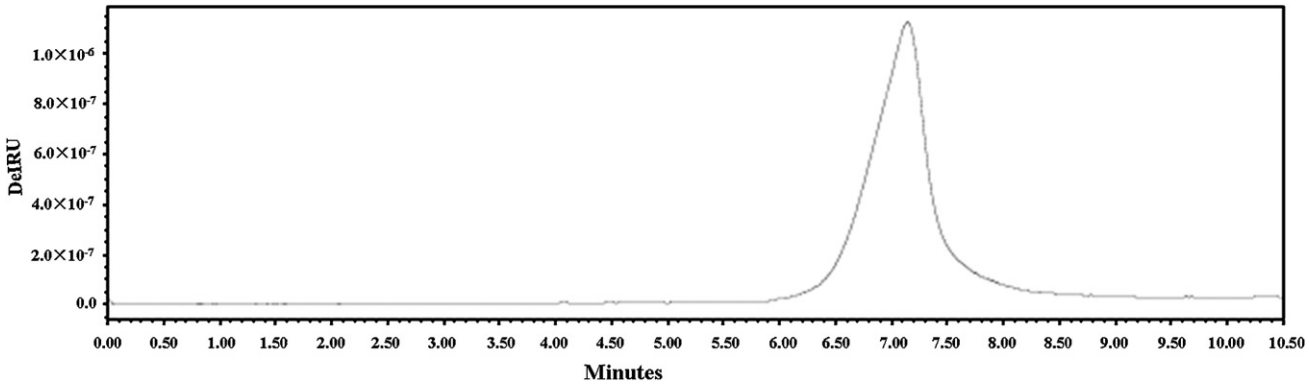


**Fig. 1.** HPLC of F21 on TSK-gel PW superoligo column. The void volume of the column is approximately 1.6 mL and the total column volume is 4.3 mL.

## 3. Results and discussion

### 3.1. Yield and monosaccharide composition of polysaccharide WL-26

The yield of purified WL-26 polysaccharide was 1.26 g, and monosaccharide compositional analysis indicated the presence of L-rhamnose, D-glucose, D-mannose, D-galactose, and D-glucuronic acid in a molar ratio of 10:9:3:1:3. According to Jansson, Lindberg, Wildmalm, and Sandford, 1985, welan (S-130) contained glucose, rhamnose and mannose in the relative proportions 43:46:11, as well as glucuronic acid (Jansson et al., 1985). The absence of an absorption peak at 280 nm indicated that WL-26 contained no protein.

### 3.2. Composition of F21

HPLC of F21 produced a single symmetrical peak, indicating it was a homogeneous oligosaccharide (Fig. 1) with a molecular weight of $\sim 1.4 \times 10^3$ Da based on a calibration curve prepared with dextran and oligosaccharide standards. Lack of absorption at 280 nm indicated that F21 contained no protein.

Infrared spectroscopy revealed characteristic peaks at 3427, 2920, 1618, 1416, 1157, 1047 and 617 $cm^{-1}$. The broad absorption band at 3427 $cm^{-1}$ is representative of the stretching frequency of —OH groups and the intermolecular H-bridges between the OH groups, and the band at 2920 $cm^{-1}$ is attributable to $CH_2$ asymmetric stretching. The relative absorption peaks at 1618 $cm^{-1}$ and 1416 $cm^{-1}$ are also characteristic of polysaccharides, and the region 1200–1000 $cm^{-1}$ contained three absorption peaks indicative of a pyranan saccharide (Ge, Zhang, & Sun, 2009). A weak absorption peak at 1730 $cm^{-1}$ indicated the presence of uronic acids.

Monosaccharide compositional analysis of F21 indicated the presence of L-rhamnose, D-glucose, D-mannose, D-galactose, and glucuronic acid in a molar ratio of 3:1.7:1:1:0.7.

### 3.3. Structural characterization of F21

GC–MS data (Table 1) indicated F21 to be a branched structure with the main chain consisting of 1,4,6-tri-substituted glucose, 1,4-di-substituted rhamnose, 1,3-di-substituted glucose and 1,4-di-substituted mannose, and to contain a terminal side-chain galactose substituent attached to the 1,4,6-tri-substituted glucose residue. Minor amounts of terminal glucose and rhamnose residues were also identified. NMR analysis suggested the presence of D-glucuronic acid residues distributed at the non-reducing terminal of the main chain.

$^1$H NMR spectra (Fig. 2) revealed seven anomeric signals of similar intensity occurring at $\delta$ 5.26 ($J_{H\text{-}1,H\text{-}2} \leq 3$ Hz), $\delta$ 5.14 (br.s), $\delta$ 4.90 (br.s), $\delta$ 4.79 ($J_{H\text{-}1,H\text{-}2} \sim 8$ Hz), $\delta$ 4.70 ($J_{H\text{-}1,H\text{-}2} \sim 8$ Hz), $\delta$ 4.569 (br.s) and $\delta$ 4.553 (br.s) indicating a regular oligosaccharide unit (A–G, in decreasing chemical shift order), one $CH_3$-group (H-6 of Rha) at $\delta$ 1.39 ($J_{5,6} \sim 7$ Hz), and a minor $CH_3$-group (H-6 of Rha) signal at 1.37 ($J_{5,6} \sim 7.0$ Hz), Other sugar protons were observed in the $\delta$ 3.34–4.00 region. Both chemical shifts and vicinal coupling constant values were in good agreement with an α-anomeric configuration for the first two residues. The $^{13}$C NMR spectrum (Fig. 3) of the oligosaccharide contained signals for seven anomeric carbons ($\delta$ 94.50, $\delta$ 96.43, $\delta$ 96.08, $\delta$ 105.61, $\delta$ 98.42, $\delta$ 104.96 and $\delta$ 105.07), two $CH_3$—C groups (C-6 of Rha) at $\delta$ 19.60, and sugar ring carbons linked to oxygen in the $\delta$ 62.77–83.93 region, together with one CO group at $\delta$ 178.11.

Using published methodology (Duus, Gotfredsen, & Bock, 2000; Hounsell, 1995), the complete structural characterization of F21 were achieved following 2D NMR analysis involving COSY, TOCSY, NOESY, $^1$H–$^{13}$C HMQC and HMBC experiments, which were used to assign the chemical shift spin systems of the seven sugar residues present in the repeating unit (Table 2).

**Table 1**
Linkage analysis and percentage of O-methylated sugars in F21.

| Methylated sugars | Linkage | Molar ratios |
|---|---|---|
| 2,3,4,6-$Me_4$-Gal | Terminal | 1.43 |
| 2,3-$Me_2$-Glc | 1,4,6-Glc*p* | 1.21 |
| 2,4,6-$Me_3$-Glc | 1,3- Glc*p* | 1.02 |
| 2,3-$Me_2$-Rha | 1,4-Rha*p* | 2.03 |
| 2,3,6- $Me_3$-Man | 1,4-Man*p* | 1.01 |

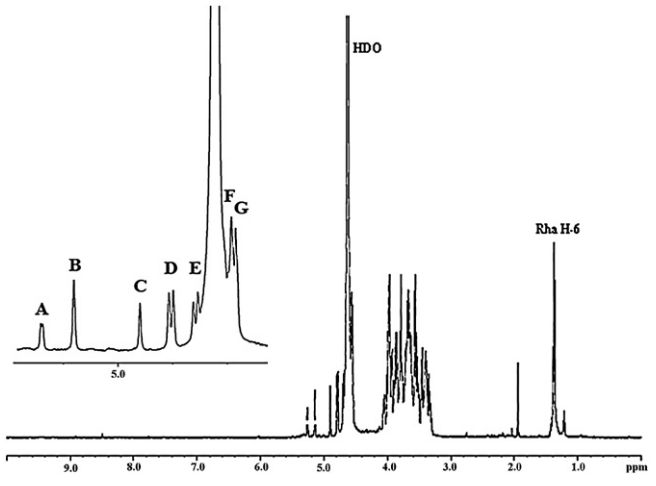


**Fig. 2.** 500 MHz $^1$H NMR spectrum of F21 in $D_2O$ at 27 °C. The anomeric protons are labeled as (A)– (G).

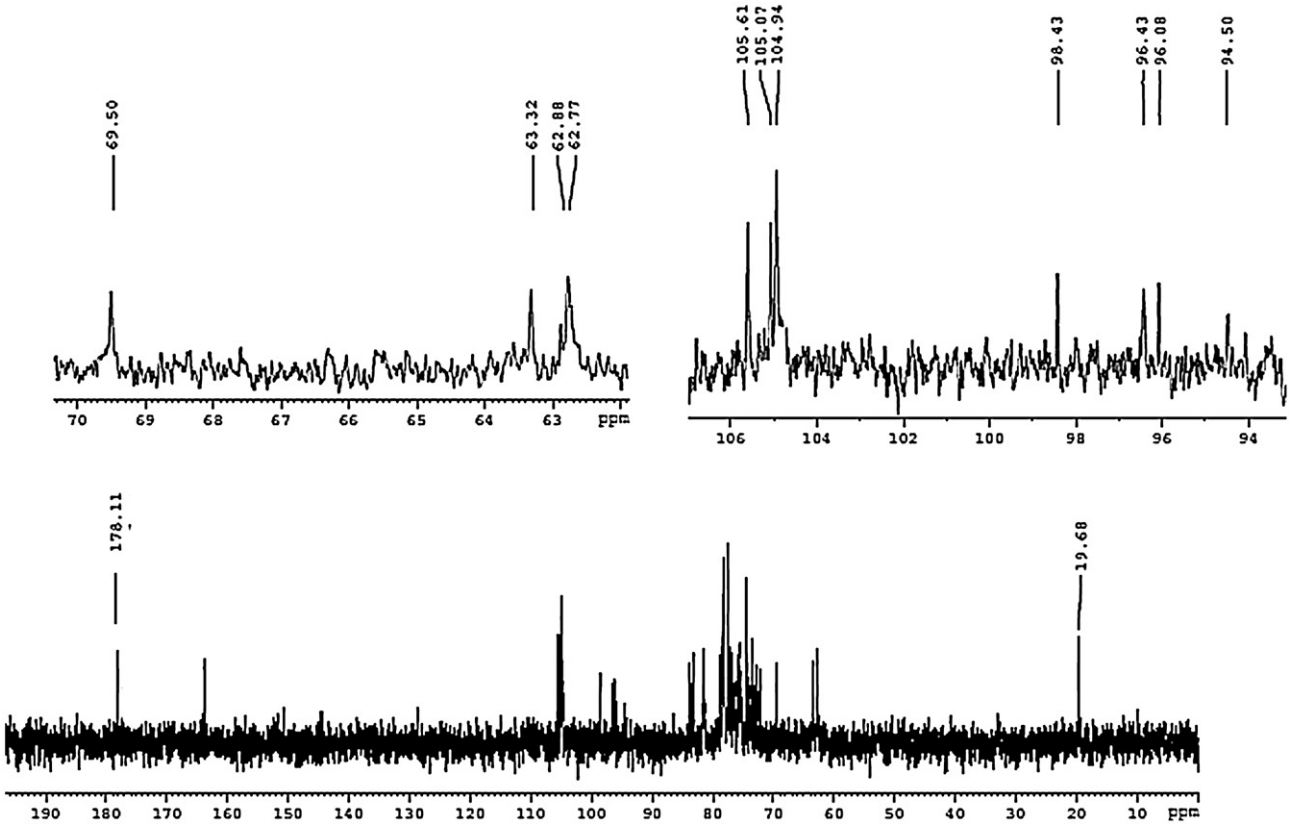


**Fig. 3.** 500 MHz $^{13}$C NMR spectrum of F21 in $D_2O$ at 27 °C.

Chemical shifts of residue A were assigned according to COSY and TOCSY spectra. $^{13}$C resonances were assigned from the HSQC spectrum (Table 2). The small $J_{H\text{-}1,H\text{-}2}$ coupling constant in the $^1$H NMR spectrum, and the H-1/H-2 intra-residue correlations in the NOESY spectrum, indicated that residue A had an α-configuration. The downfield shifts of the C-4 ($\delta$ 81.37) and C-6 ($\delta$ 69.50) carbon signals with respect to standard values for glucopyranoses indicate that residue A was 1,4,6-α-D-Glc*p*. HMBC experiments (Table 4) showed clear correlations between H-1 of residue A and C-4 of residue G indicating that residue A was linked with residue G by a 1,4-O glycosidic bond.

$^1$H resonances for H-1 to H-4 of residue B were assigned from the cross-peaks in COSY and TOCSY spectra. The COSY spectrum showed most of the correlations between the neighboring protons within each spin system, but there was no H-4, H-5 correlation. The signals from H-1 to H-3 of residues B are coincident and diverge from H-4. The H-5 resonance was assigned from the H-3/H-4 and H-4/H-5 cross-peaks in the NOESY spectrum. H-5, H6a and H-6b were assigned from the TOCSY spectrum. In the HMBC spectrum, the cross-peaks of H-1 and C-3, C-5 showed that H-5 and H-6 are located on residue B. The chemical shifts of C-1 to C-6 were readily obtained from the HMQC spectrum (Table 2). A self-spin system

**Table 2**
$^1$H and $^{13}$C NMR chemical shifts (ppm) of F21 at 27 °C.

| Residue | Proton or carbon | | | | | |
|---|---|---|---|---|---|---|
| | H-1/C-1 | H-2/C-2 | H-3/C-3 | H-4/C-4 | H-5/C-5 | H-6/C-6 |
| A →4,6)-α-D-Glc*p*-(1→ | 5.26<br>94.5 | 3.62<br>77.47 | 3.98<br>72.65 | 3.64<br>81.37 | 3.85<br>75.43 | 3.97[a], 3.98[a]<br>69.50 |
| B α-D-Gal*p*-(1→ | 5.14<br>96.43 | 3.97<br>73.55 | 4.04<br>72.65 | 3.87<br>78.07 | 3.92<br>78.07 | 3.86[a], 3.93[b]<br>63.32 |
| C →4)-α-D-Man*p*-(1→ | 4.90<br>96.08 | 3.97<br>72.65 | 3.87<br>73.92 | 3.67<br>81.49 | 3.86<br>73.22 | 4.01[a], 3.90[b]<br>62.77 |
| D → 3) - α-L-Rha*p* | 4.80<br>105.61 | 3.40<br>75.43 | 3.72<br>83.92 | 3.71<br>76.89 | 3.97<br>69.50 | 1.37<br>19.71 |
| E β-D-GlcA-(1→ | 4.70<br>98.42 | 3.32<br>76.30 | 3.68<br>76.89 | 3.66<br>78.07 | 3.81<br>77.47 | <br>178.11 |
| F →3)-β-D-Glc*p*-(1→ | 4.56<br>104.94 | 3.36<br>76.30 | 3.53<br>78.23 | 3.43<br>75.36 | 3.71<br>76.89 | 4.05, 3.96<br>62.88 |
| G →4)-β-L-Rha*p*-(1→ | 4.55<br>105.07 | 3.41<br>75.66 | 3.57<br>78.07 | 3.79<br>83.07 | 3.55<br>78.07 | 1.39<br>19.71 |

[a] Chemical shift for H-6a.
[b] Chemical shift for H-6b.

**Table 3**
Inter-glycosidic correlations from NOESY spectra of F21.

| Residue | Proton | Intra-correlation |
|---|---|---|
| A →4,6)-α-D-Glc*p*-(1→ | 5.26 (H-1) | 3.62 (A: H-2) |
| B α-D-Gal*p*-(1→ | 5.14 (H-1) | 3.97 (B: H-2) |
| | 3.87 (H-4) | 4.04 (B: H-3), 3.87 (B: H-4), 3.92 (B: H-5) |
| C →4)-α-D-Man*p*-(1→ | 4.90 (H-1) | **3.53 (F: H-3)**, 3.87 (C: H-3), 3.97 (C: H-2) |
| D →3)-α-L-Rha*p* | 4.80 (H-1) | 3.72 (D: H-3), 3.71 (D: H-4), 3.40 (D: H-2) |
| E β-D-GlcA-(1→ | 4.70 (H-1) | 3.32 (E: H-2), 3.66 (E: H-4), **3.64 (A: H-4)** |
| F →3)-β-D-Glc*p*-(1→ | 4.56 (H-1) | 3.45 (F: H-2), 3.92 (F: H-5) |
| G →4)-β-L-Rha*p*-(1→ | 4.55 (H-1) | 3.55 (G: H-5), **3.67 (C: H-4)**, 3.79 (G: H-4) |

Inter-residue NOESY are shown in bold font.

from H-1 to H-3, the large coupling constant value $J_{H\text{-}2,H\text{-}3}$ (~9 Hz), and the small coupling constant value $J_{H\text{-}4,H\text{-}5}$ (<3.0 Hz) indicated that residue B was galactopyranose. The anomeric signal at $\delta$ 5.14 and the small $J_{H\text{-}1,H\text{-}2}$ value in the $^1$H NMR spectrum, and H-1/H-2 intra residue correlations in the NOESY spectrum, indicated that residue B was α-D-Gal*p*. HMBC experiments (Table 4) showed clear correlations between H-1 of residue B and C-6 of residue A indicating that residue B was linked with residue A by a 1,6-O glycosidic bond.

$^1$H resonances for H-1, H-2, H-3 and H-4 of residue C were assigned from the cross-peaks in the COSY and TOCSY spectra. H-5, H-6a and H-6b were assigned from the COSY, TOCSY and HMBC spectra. The carbon chemical shifts from C-1 to C-6 were assigned from the HSQC spectrum (Table 2). Identification of the mannopyranose residue C signals was based on the small value of $J_{H\text{-}1,H\text{-}2}$ < 3 Hz and the large coupling constant value of $J_{H\text{-}4,H\text{-}5}$ (~8 Hz). The small $J_{H\text{-}1,H\text{-}2}$ value for the D-mannosyl residue did not provide information about the anomeric configuration (Paramonov, Bailey, Rangarajan, Hashim, Kelly, & Curtis, 2001). The α configuration of Man was inferred from the H-5 and C-5 chemical shifts at $\delta$ H-5 3.86 and $\delta$ C-5 73.2; published values for α-mannopyranose are $\delta$ H-5 3.82 and $\delta$ C-5 73.34, and $\delta$ H 3.38, and $\delta$ C 77.00 for β-mannopyranose (Jansson, Kenne, & Widmalm, 1989). The downfield shift of the C-4 ($\delta$ 81.49) carbon signal with respect to standard values for mannopyranose indicate that residue C was (1→4)-α-D-Man*p* (Senchenkova, Knirel, Shashkova, Ahmed, Mavridis, & Rudolph, 2003). Inter-residue NOE correlations (Table 3) were observed between H-1 of residue C and H-3 of residue F indicating that residue C was linked with residue F by a 1,3-O glycosidic bond.

$^1$H resonances (H-1 $\delta$ 4.80 and H-6 $\delta$ 1.37) for residue D were characteristic of a 6-deoxysugar, which was identified as Rha (Perry, Bundle, MacLean, Perry, & Griffith, 1986). The α-configuration of Rha was established from the chemical shift of the C-5 signal at $\delta$ 69.50; published values for C-5 in α-Rha*p* and β-Rha*p* are $\delta$ 70.0 and $\delta$ 73.2, respectively (Bradbury & Jenkins, 1984; Jansson et al., 1989). The downfield shifts of the C-3 ($\delta$ 83.92) carbon signal with respect to standard values for α-L-rhamnopyranoside indicated that residue D was →3)-α-L-Rha*p*.

Chemical shifts of residue E were assigned according to COSY and TOCSY spectra. The carbon chemical shifts from C-1 to C-6 were assigned from the HMQC spectrum (Table 2). The large $J_{H\text{-}1,H\text{-}2}$ coupling constant (~8 Hz) indicated that residue E had the β-configuration, and the chemical shift of the C-6 signal at $\delta$ 178.11 identified residue E as β-D-GlcA. Inter-residue NOE correlations (Table 3) were observed between H-1 of residue E and H-4 of residue A indicating that residue E was linked with residue A by a 1,4-O glycosidic bond.

The anomeric signal at $\delta$ 4.56 indicated that residue F was a β-linked residue. Proton chemical shifts from H-2 to H-6 were assigned from 2D NMR, including COSY, TOCSY, NOESY, HMBC and HSQC spectra. The large $J_{2,3}$ value and $J_{3,4}$ coupling constants (9 Hz) indicated that residue F was D-glucopyranose. The downfield shift of the C-3 ($\delta$ 78.23) carbon signal indicated that residue F was (1→3)-β-D-Glc*p*. HMBC experiments (Table 4) showed clear correlations between H-1 of residue F and C-4 of residue G indicating that residue F was linked with residue G by a 1,4-O glycosidic bond.

$^1$H resonances for residue G (H-1 $\delta$ 4.55, H-6 $\delta$ 1.39) were characteristic of a 6-deoxysugar, which was identified as Rha. The β-configuration of the Rha residue was established from the chemical shift of the C-5 signal at $\delta$ 78.07; published values for C-5 in α-Rha*p* and β-Rha*p* are $\delta$ 70.0 and $\delta$ 73.2, respectively. The downfield shift of the C-4 ($\delta$ 83.07) carbon signal with respect to standard values for glucopyranoses indicated that residue G was (1→4)-β-L-Rha*p*. HMBC experiments (Table 4) showed clear correlations between H-1 of residue G and C-3 of residue D, and between H-1 of residue G and C-4 of residue C. Inter-residue NOE correlations (Table 3) were observed between H-1 of residue G and H-4 of residue C indicating that residue G was linked with residue D by a 1,3-O glycosidic bond and with residue C by a 1,4-O glycosidic bond.

The sequence of the glycosyl residues was determined from NOESY studies followed by confirmation with HMBC experiments. Based on the data presented above, F21 has the following

**Table 4**
Inter-glycosidic correlations from of F21.

| Residue | Proton | Proton correlation |
|---|---|---|
| A →4,6)-α-D-Glc*p*-(1→ | 5.26 (H-1) | **83.07 (G: C-4)** |
| B α-D-Gal*p*-(1→ | 5.14 (H-1) | **69.50 (A: C-6)**, 72.65 (B: C-3) |
| C →4)-α-D-Man*p*-(1→ | 4.90 (H-1) | 73.92 (C: C-3) |
| D →3)-α-L-Rha*p* | 4.80 (H-1) | 69.50 (D:C-5), 83. 92 (D: C-3) |
| E β-D-GlcA-(1→ | 4.70 (H-1) | |
| F →3)-β-D-Glc*p*-(1→ | 4.56 (H-1) | **83.07 (G: C-4)** |
| G →4)-β-L-Rha*p*-(1→ | 4.55 (H-1) | 75.66 (H: C-2), **81.49 (C: C-4)**, 83.07 (G: C-4), **83.92 (D: C-3)** |

Proton correlation HMBC spectra are shown in bold font.

structure:

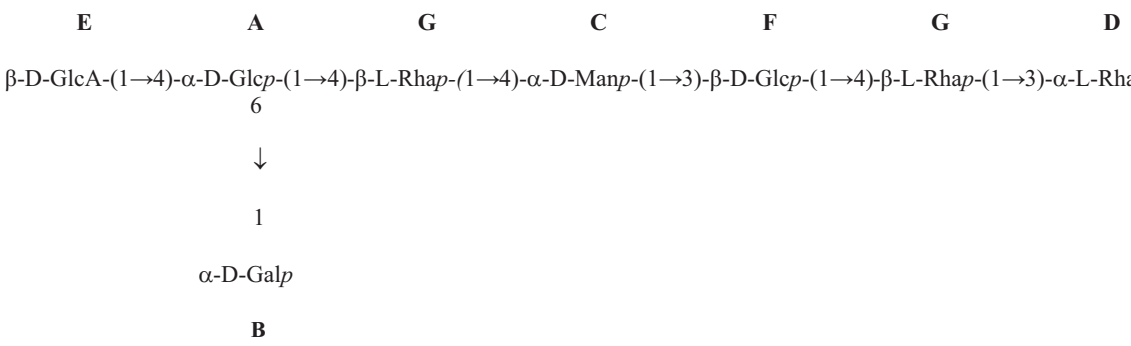


## 4. Conclusions

An oligosaccharide, F21, was purified by Sephacryl S-100 gel chromatography following partial acid hydrolysis of exopolysaccharide WL-26, produced by a *Sphingomonas* sp., with 0.2 M trifluoroacetic acid. Compositional analysis showed that the oligosaccharide is composed of glucose, rhamnose, galacotose, mannose and GlcA. Linkage analysis and $^{1}H$ and $^{13}C$ and 2D NMR spectroscopy established that F21 consisted of:

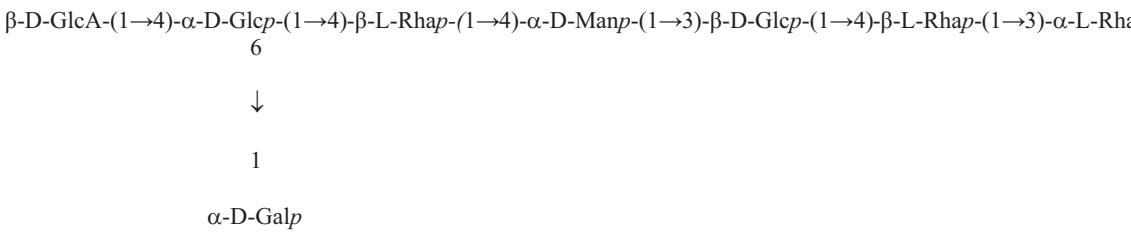


The deduced molecular weight based on the proposed structure is 1280 Da compared with the 1400 Da value determined experimentally by HPLC.

These findings provide new insight into the structure of polysaccharide WL-26.

## Acknowledgements

We thank Ms. Li-ping Shi of the Shanghai Institute of Organic Chemistry, Chinese Academy of Sciences for valuable assistance, and Dr. John Buswell of the Institute of Edible Fungi, Shanghai Academy of Agricultural Sciences for linguistic revision of the manuscript. This work was supported by the Shanghai Committee of Science and Technology, China (Grant No. 054319940), National Natural Science Foundation of China (Grant No. 31171640), and National High-tech R&D Program, China(Grant No. 2011BAD23B04, 2012AA021201, and 2012AA021505).

## References

Albersheim, P., Nevins, D. J., English, P. D., & Karr, A. (1967). A method for analysis of sugars in plant cell wall polysaccharides by gas chromatography. *Carbohydrate Research*, *5*, 340–345.

Anumula, K. R., & Taylor, P. B. (1992). A comprehensive procedure for preparation of partially methylated alditol acetates from glycoprotein carbohydrates. *Analytical Biochemistry*, *203*, 101–108.

Balsara, N. P., Fetters, L. J., Hadjichristidis, N., Lohse, D. J., Han, C. C., Graessley, W. W., et al. (1992). Thermodynamic interactions in model polyolefin blends obtained by small-angle neutron scattering. *Macromolecules*, *25*, 6137–6147.

Bradbury, J. H., & Jenkins, G. A. (1984). Determination of the structures of trisaccharides by 13C-n.m.r. spectroscopy. *Carbohydrate Research*, *126*, 125–156.

Duus, J., Gotfredsen, C. H., & Bock, K. (2000). Carbohydrate structural determination by NMR spectroscopy: Modern methods and limitations. *Chemical Reviews*, *100*, 4589–4614.

Ge, Q., Zhang, A. Q., & Sun, P. L. (2009). Structural investigation of a novel water soluble heteropolysaccharide from the fruiting bodies of *Phellinus baumii* Pilát. *Food Chemistry*, *114*, 391–395.

Hounsell, E. F. (1995). $^{1}H$ NMR in the structural and conformational analysis of oligosaccharides and glycoconjugates. *Progress in Nuclear Magnetic Resonance Spectroscopy*, *27*, 445–474.

Jansson, P. E., Kenne, L., & Widmalm, G. (1989). Computer-assisted structural-analysis of polysaccharides with an extended version of CASPER using 1H-NMR and 13C-NMR data. *Carbohydrate Research*, *188*, 169–191.

Jansson, P.-E., Kumar, N. S., & Lindberg, B. (1986). Structural studies of a polysaccharide (S-88) elaborated by *Pseudomonas* ATCC 31554. *Carbohydrate Research*, *156*, 165–172.

Jansson, P. E., Lindberg, B., Widmalm, G., & Sandford, P. A. (1985). Structural studies of an extracellular polysaccharide (S-130) elaborated by Alcaligenes ATCC 31555. *Carbohydrate Research*, *139*, 217–223.

Jansson, P.-E., Lindberg, B., & Sandford, P. A. (1983). Structural studies of gellan gum, an extracellular polysaccharide elaborated by *Pseudomonas elodea*. *Carbohydrate Research*, *124*, 135–139.

Jansson, P. E., & Widmalm, G. (1994). Welan gum (S-130) contains repeating units with randomly distributed L-mannosyl and L-rhamnosyl terminal groups, as determined by FABMS. *Carbohydrate Research*, *256*, 327–330.

Kuo, M. S., Mort, A. J., & Dell, A. (1986). Identification and location of L-glycerate, an unusual substituent in gellan gum. *Carbohydrate Research*, *56*, 73–187.

Kwon, B. D., Foss, P. A., & Rha, C. (1987). Rheological characterization of high viscosity polysaccharides. In M. Yalpani (Ed.), *Industrial polysaccharides – Proceedings of the symposium on the applications and modifications of industrial polysaccharides: Genetic engineering, structure/property relations, and applications* (pp. 253–266). Amsterdam: Elsevier Science Publishers.

Madras, G., & Chattopadhyay, S. (2001). Effect of benzoyl peroxide on the ultrasonic degradation of poly (vinyl acetate). *Polymer Degradation and Stability*, *73*, 33–38.

Paramonov, N., Bailey, D., Rangarajan, M., Hashim, A., Kelly, G., Curtis, M. A., et al. (2001). Structure analysis of the polysaccharide from the lipopolysaccharide of *Porphyromonas gingivalis* strain W50. *European Journal of Biochemistry*, *268*, 4698–4707.

Perry, M. B., Bundle, D. R., MacLean, L., Perry, J. A., & Griffith, D. W. (1986). The structure of the antigenic lipopolysaccharide O-chains produced by *Salmonella urbana* and *Salmonella godesberg*. *Carbohydrate Research*, *156*, 107–122.

Podolsak, A. K., Tiu, C., Saeki, T., & Usui, H. (1996). Rheological properties and some applications for rhamsan and xanthan gum solutions. *Polymer International*, *40*, 155–167.

Pollock, T. J. (2002). Sphingan group of exopolysaccharides (EPS). In E. J. Vandamme, S. DeBaets, & A. Steinbüchel (Eds.), *Biopolymers-polysaccharides I* (pp. 239–258). Weinheim: Wiley-VCH.

Senchenkova, S. N., Knirel, Y. A., Shashkova, A. S., Ahmed, M., Mavridis, A., & Rudolph, K. (2003). Structure of the O-polysaccharide of *Erwinia carotovora* ssp. carotovora GSPB 436. *Carbohydrate Research*, *338*, 2025–2027.

Yang, R. Z., Zhang, J. S., Tang, Q. J., & Pan, Y. J. (2005). High performance anion exchange chromatography method to determine the monosaccharide composition of polysaccharide. *Edible Fungi of China*, *24*, 42–44 (in Chinese).